HHS Public Access

Author manuscript

J Immunol. Author manuscript; available in PMC 2021 March 01.

Published in final edited form as:

J Immunol. 2020 March 01; 204(5): 1091–1100. doi:10.4049/jimmunol.1900501.

Abrogated AID function prolongs survival and diminishes renal pathology in the BXSB mouse model of SLE

Jing Zhu[1], **Alayna N Hay**[1], **Ashley A Potter**[1], **Madison W Richwine**[1], **Thomas Sproule**[2], **Tanya LeRoith**[3], **John Wilson**[2], **Muneer G Hasham**[2], **Derry C Roopenian**[2], **Caroline M Leeth**[1]

[1]Department of Animal and Poultry Sciences, Virginia Tech, Blacksburg, VA 24061

[2]The Jackson Laboratory, Bar Harbor, ME 04609

[3]Department of Biomedical Sciences and Pathobiology, Virginia-Maryland College of Veterinary Medicine, Virginia Tech, Blacksburg, 24061

Abstract

Almost a decade has passed since the approval of belimumab, a monoclonal antibody directed against B lymphocyte stimulation and the first targeted therapy approved for systemic lupus erythematous (SLE) in over 50 years. While well tolerated, the efficacy of belimumab remains limited and is not labelled for patients suffering from nephritis, the leading cause of patient mortality. We sought to explore alternative targets of autoreactive B lymphocytes through manipulation of affinity maturation. The BXSB/MpJ mouse, a well-established model of human SLE, develops elevated antinuclear antibodies and immune complex-mediated nephritis along with other manifestations of SLE-like disease. To limit interfering with critical background genetics, we used CRISPR-Cas9 to disrupt *Activation Induced Cytidine Deaminase* (*Aicda*, AID) directly in BXSB zygotes. Homozygous null mice demonstrated significantly prolonged survival compared to wildtype. While mice continued to develop plasma cells, splenic follicular structure was restored and renal pathology was reduced. Mice developed expanded germinal center B lymphocyte populations as in other models of AID deficiency as well as increased populations of $CD73^+$ B lymphocytes. Treatment with the small molecule inhibitor of RAD51, 4,4'-Diisothiocyano-2,2'-stilbenedisulfonic acid, resulted in minimal changes in disease markers in BXSB mice. The prolonged survival in AID-deficient BXSB mice appears attributed primarily to the reduced renal pathology, warranting further exploration as current therapeutics targeting lupus nephritis are limited and thus in great demand.

INTRODUCTION

Systemic lupus erythematosus (SLE) is a complex, B lymphocyte–driven autoimmune disease in which high levels of circulating autoreactive antibodies exert toxic effects that lead to organ damage, most significantly severe nephritis. SLE has no effective cure and current treatments are based on global immunosuppression, often insufficiently controling symptoms coupled with significant side effects. Advances in therapeutics for SLE have been slow with the notable exception of belimumab, a monoclonal antibody targeting B lymphocytes, which became the first FDA-approved drug for SLE in decades (1–3). The success of belimumab establishes the clinical effectiveness of targeting pathogenic B lymphocytes in SLE; however, only ~30% of lupus patients benefited from this treatment in

clinical trials (Arthritis Advisory Committee Meeting, 16 Nov 2010) with no current labelling for patients with nephritis. This warrants further investigations into novel therapeutics targeting B lymphocytes for lupus patients.

A defining hallmark of SLE is the presence of copious amounts of antinuclear autoantibodies (ANA) generated by autoreactive B lymphocytes (4, 5). The accumulation of ANA and other autoantibodies results in the formation of immune complexes that activate downstream effector mechanisms, including the fixation of complement, activation of monocytes, and the abundant secretion of proinflammatory cytokines, most notably type-1 interferons (6, 7). These events ultimately lead to multi-system organ erosion, in particular renal failure which is the leading cause of death among SLE patients (8). The majority of pathogenic autoantibodies in human patients with SLE are highly mutated and isotype switched from IgM and IgD to IgG (4, 5). This indicates the autoantibodies are produced by affinity matured B lymphocytes which have undergone class switch recombination (CSR) and somatic hypermutation (SH). Both CSR and SH are driven by activation-induced cytidine deaminase (AID), an enzyme that initiates double-stranded DNA breaks (DSB) predominantly in immunoglobulin genes (9–13). These DSB are then repaired via homologous recombination (HR) by the RAD51 protein family(14–19). Failure to repair DSB leads to cell apoptosis and loss of CSR, thus providing a potential approach for disrupting CSR and abrogating pathogenic autoantibody production (20).

AID is expressed principally in B lymphocytes residing within germinal centers (Immgen.org) and its expression is increased in the MRL/MpJ-Fas^{lpr}/J (MRL/lpr) mouse model of SLE (21). Previous studies show disrupting CSR through introduction of an *Aicda* null gene in MRL/lpr mice results in marked reduction in disease symptoms, including decreased nephritis and decreased levels of IgG autoantibodies, leading to increased survival (22). These mice also had high levels of autoreactive IgM that exerted a protective effect (23), suggesting that preservation of circulating IgM may be beneficial. However, when *Aicda* was knocked out in C57BL/6 mice carrying the *lpr* mutation, SLE-like disease was rapidly accelerated, driven by autoreactive IgM antibodies (24). These conflicting studies raise the important question of whether IgM autoantibodies can substitute for their IgG counterparts in the development of SLE. The BXSB/MpJ mouse offers a model in which SLE-like disease develops through the effects of multiple SLE genetic loci and duplicated expression of *Tlr7* (25, 26). This model exhibits a spontaneous, robust extrafollicular response with reduced marginal B lymphocyte numbers and copious plasma cell generation (27, 28). BXSB mice, with a disease pathogenesis distinct from MRL/lpr mice, provide a good model to resolve controversy regarding the role of AID in SLE development.

In this study, we utilized CRISPR-Cas gene editing techniques to ablate AID expression directly in the BXSB background. This technique allowed for gene targeting with minimal disrupt to background genetics critical for the study of complex traits. We found SLE-like disease diminished in BXSB mice lacking AID with significant improvements in lupus nephritis, a rebound in marginal zone B lymphocyte populations and a restoration of splenic and germinal center architecture. We then investigated the ability of an inhibitor RAD51, previously found successful in limiting autoimmune disease (29), to attenuate the progression of lupus-like disease in our mice.

MATERIALS AND METHODS

Mice

Mice were maintained under specific pathogen-free conditions with the approval of the Institutional Animal Care and Use Committee of Virginia Tech. BXSB/MpJ mice (henceforth referred to as "BXSB") were provided by Dr. D. Roopenian (JR000740, available from the Jackson Laboratory). BXSB.*Aicda*$^{-/-}$ mice were generated using CRISPR-Cas 9 technology as described (29). Briefly, the following single-guide RNAs were used to target *Aicda* exon 1 or 2 respectively : 5'-gaaattaatacgactcactataggAGTCACGCTGGAGAC-CGATAgttttagagctagaaatagc-3' or 5'-gaaattaatacgactcactataggACTTCTTTTGCTTC-ATCAGAgttttagagctagaaatagc-3' (the uppercase letters being the complementary sequences to the targeted region). The resulting progeny were backcrossed to wt BXSB mice. N1 progeny were sequenced and a founder with a 101bp deletion on exon 1 was identified. This founder was backcrossed one additional time to BXSB to further reduce the chance of off-target effects with the resulting progeny then intercrossed to homozygosity. The line was maintained by brother sister matings (referred to as BXSB.*Aicda*$^{-/-}$ in the text). Genotyping primers (Intergrated DNA Technologies) used for *Aicda* were forward, 5'–TCACACAACAGCACTGAAGC–3'; and reverse, 5'–ACCCAAA-AGACCTGAGCAGA–3'. PCR products were run on a 1.5% agarose (Lonza) gel and imaged on ChemiDoc XRS+ (BioRad) using Image Lab software. The band size for wildtype is 230bp and for *Aicda* knockout is 129bp. Ear pinna collected at the time of notching for identification was used for genotyping.

In vitro CSR assay

Splenocytes from 8–9 weeks old BXSB and BXSB.*Aicda*$^{-/-}$ male mice were treated with ACK lysis buffer and then incubated with biotin-CD43 (S7, BD Biosciences) for 30 min at 4 C followed by streptavidin microbeads (Miltenyi Biotec) for 15min at 4 C. Cells were washed and passed through MACS LD columns (Milteni Biotec) according to the manufacturer's instructions. Enriched B lymphocytes were resuspended at 1×10^6/mL in X-VIVO (Lonza) supplemented with 2-ME (Sigma). Cells were then stimulated with IL4 (50ng/mL, Peprotech) and anti-CD40 (2μg/mL, HM40–3 BD Biosciences) at 37 C (5% CO_2) for 48h. After 48h, cells were re-stimulated with IL4 (25ng/mL) and anti-CD40(1μg/mL). At 96h, cells were incubated with anti-IgG1(A85–1, BD Biosciences) for 30 minutes at 4 C and collected on an Attune NxT cytometer (Thermo Fisher Scientific). Results were analyzed using Flowjo software (Flowjo LLC).

RT PCR

Splenocytes were isolated from 12–15 week old BXSB and BXSB.*Aicda*$^{-/-}$ males and enriched for B lymphocytes as described in CSR assay. These B lymphocytes were resuspended at 1×10^6/mL in X-VIVO (Lonza) supplemented with 2-ME (Sigma). Cells were then stimulated with IL4 (10ng/mL, Peprotech) and anti-CD40 (0.1μg/mL, HM40–3 BD Biosciences) at 37 C (5% CO_2) for 72h. Cells were harvested for RNA extraction using Quick-RNA MicroPrep Kit (Zymo Research, cat. ZR1050). cDNA was synthesized using High Capacity cDNA Reverse Transcription Kit (Thermo Fisher, cat. 4368813). Primers for *Aicda* RT-PCR are 5'-CAGGGACGGCATGAGACCT-3' and 5'-

TCAGCCTTGCGGTCTTCACA-3', and primers for *Gapdh* are 5'-GAGAAACCTGCCA AGTATGATGAC-3' and 5'-TGATGGTATTCAAGAGAGTAGGGAG-3' (29). PCR products were run on a 1.5% agarose (Lonza) gel and imaged on ChemiDoc XRS+ (BioRad) using Image Lab software. The band size for *Aicda* is 302bp and for *Gapdh* is 421bp.

In vitro plasma cell generation

Splenocytes from 8-week-old BXSB males were isolated to gain enriched B lymphocytes as described in CSR assay. Enriched B lymphocytes were stimulated with IL-4 (4ng/mL, Peprotech), TGF-β (2ng/mL, R&D Systems), anti-Igδ/dex (100ng/mL, Fina Biosolutions) and retinoic acid (10μM, Sigma) plus either anti-CD40 (2μg/mL, HM40–3, BD Biosciences) for T cell-dependent (TD) response or LPS (5μg/mL, Sigma) for T cell-independent (TI) response. After 66h, cells were stained with antibodies and analyzed using flow cytometry as described.

Flow cytometry

Splenocytes were treated with ACK lysis buffer. (For the 4,4'-Diisothiocyano-2,2'-stilbenedisulfonic acid (DIDS) experiments, splenocytes were not lysed since DIDS-exposed red blood cells are refractory to lysis. RBC were excluded by gating for size in those experiments.) Splenocytes and femoral bone marrow were counted using a Nexcelom cell counter and resuspended at 2×10^7 cells/mL. Cells were then stained with fluorochrome-conjugated antibodies for 30 min at 4 C and propidium iodide (Biolegend) or 7-AAD (Biolegend) was added before analyzing to differentiate live and dead cells. The following fluorchrome-conjugated antibodies (clones) were utilized: B220 (RA3–6B2), CD4 (GK1.5), CD8 (53–6.7), CD21 (7E9), CD23 (B3B4), GL7 (GL7), CD73 (TY/11.8), CD138 (281–2), CD11b (M1/70), CXCR5 (L138D7), ICOS (C398.4A), PD-1 (RMP1–30), (Biolegend); FAS(Jo2), IgG1(A85–1), (BD Biosciences). Apoptosis was characterized using Apoptosis Kit (Biolegend) following the manufacturer's instructions. All experiments were performed on an Attune NxT cytometer (Thermo Fisher Scientific) and data were analyzed using FlowJo software (Flowjo LLC). All analyses were done after gating on single cells.

ANA analysis

Anti-nuclear antibodies in the sera were detected using an ANA Test Kit (Antibodies Incorporated). Either FITC anti-mouse kappa light chain (187.1, BD Biosciences) or FITC anti-mouse IgM (RMM-1, Biolegend) was used as secondary antibody. Slides were imaged with an Eclipse T*i* microscope using NIS-Elements software (Nikon). Intensity was measure using Image J software (NIH).

Urine albumin and creatinine assay

Free catch urine samples were collected from BXSB (n=8) and BXSB.*Aicda*$^{-/-}$ (n=6) males at 6 and 16 weeks of age. Samples were stored at −20°C until processed using the mouse albumin ELISA kit (Bethyl Laboratories, cat. E99–134) and creatinine colorimetric assay kit (Cayman Chemical, cat. 500701) per manufacturer's instructions. The albumin to creatinine ratio (ACR) was calculated by dividing albumin concentration in milligrams per deciliter by creatinine concentration in milligrams per deciliter.

Sera antibody ELISA

Different antibody isotypes were quantified by ELISA as described (30). Briefly, plates were incubated with appropriate coating antibody at 4 C overnight, diluted sera were added to the plate and incubated for 1h at RT followed by detection antibodies for 1h at RT. Anti-dsDNA antibodies were quantified as described (31). The plate was coated with calf thymus DNA (Sigma) at 4 C overnight. After blocking for 1h at RT, diluted sera were added to the plate and incubated for 1h at RT followed by detection antibodies for 1h at RT. Detection antibodies used in this study were either goat anti-mouse kappa chain (polyclonal, SouthernBiotech) or anti-mouse IgM (polyclonal, Bethyl) conjugated to alkaline phosphatase. Plates were developed with 1 Step PNPP (Thermo Scientific) and read on an Infinite M200 Pro plate reader using Magellan 7.0 software (Tecan).

Immunofluorescence Staining

Tissues were embedded in OCT (Thermo Scientific), frozen on dry ice for 10 min and stored at −80°C until processing. Frozen tissues were cut to 8μm using a Microm HM550 cryostat (Thermo Scientific). Slides were fixed with acetone (cat. A18–4, Fisher Chemical) at −20°C for 10 min and washed with PBS (Gibco) for 3 times. PAP pen (MilliporeSigma) was used to circle the sections and blocking buffer (3% FBS, Hyclone, Fisher) was added onto the slides and incubated in a moist chamber for over 1h. Slides were washed with PBS for 3 times and incubated with fluorochrome-conjugated antibodies against B220 (RA3–6B2), CD4 (RM4–5), CD73 (TY/11.8), GL7 (GL7), (all from Biolegend); kappa chain (187.1) (from BD Biosciences) and C3c (polyclonal, Nordic MUbio) at RT for 1h. CD16/32 (93, Biolegend) was used for Fc Block prior to Ig labeling for 30 minutes at RT. DAPI was used for nuclear counterstaining. Slides were imaged using a LSM 880 Confocal or Zeiss Axio Observer (Zeiss) microscope.

Renal pathology

Kidneys were fixed in 10% formaldehyde (Fisher Chemical) overnight and transferred to 70% ethanol (Decon Laboratories). Samples were sent to Histo-Scientific Research Laboratories for processing and H&E staining. The sections were analyzed in a blinded fashion and scored as described by a training pathologist (32). Briefly, kidneys were scored for the severity of glomerular mesangial proliferation and immune complex deposition, tubular degeneration with protein casts, interstitial inflammation, and vasculitis.

ELISPOT

ELISPOT for dsDNA producing plasma cells was performed as described (33). Briefly, ELISPOT MultiScreen plates (Millipore, cat. MSIPS4W10) were pre-coated with 10μg/mL methylated BSA (Sigma) at 37 C for 2h followed by 10μg/mL calf thymus double stranded DNA (Sigma) or PBS (control group) at 4 C overnight. Femurs and spleen were collected from 12-week-old BXSB (n=5) and BXSB.*Aicda*$^{-/-}$ (n=6) males. Bone marrow cells were flushed using syringes and resuspended at 5×10^6/mL in RPMI (Gibco) supplemented with 2g/L sodium bicarbonate (Sigma), 25mM HEPES (Sigma), 2mM L-Glutamine (Sigma), 1% Penicillin-Streptomycin (Sigma), 10%FBS and 100μM 2-ME (Sigma). Splenocytes were treated with ACK lysis buffer and resuspended at 2×10^6/mL in complete RPMI. After

blocking with complete RPMI RT for 2h, cells were seeded and cultured at 37 C (5% CO_2) overnight. After washing with PBS three times and PBST three times, plates were incubated with either goat anti-mouse kappa (polyclonal, SouthernBiotech) or anti-mouse IgM (polyclonal, Bethyl) conjugated to alkaline phosphatase for 1h. Spots were developed with NBT/BCIP (Thermo Fisher) and plates were read on an automated ELISPOT reader and analyzed by the software (AID Diagnostika). The number of anti-dsDNA secreting cells was calculated by subtracting the number in the control group (no dsDNA coating) from the number in the experimental group.

4,4'-Diisothiocyano-2,2'-stilbenedisulfonic acid (DIDS) treatment

DIDS (Tocris Bioscience) was injected intraperitoneally (IP) at 50 mg/Kg DIDS beginning at 6 weeks of age in BXSB male mice. Mice were injected weekly for a total of 8 injections. DIDS was reconstituted in 0.1M potassium bicarbonate to a concentration of 0.1M and further diluted for injection in sterile PBS. Control mice received 0.1M potassium bicarbonate diluted in sterile PBS at the same injection interval.

In vitro DIDS treatment

Splenocytes from 7-week-old BXSB males (n=4) were stimulated with IL4 (50ng/mL, Peprotech) and anti-CD40 (0.2μg/mL, HM40–3 BD Biosciences) in the presence of DIDS (TOCRIS) (0, 50, 100, 150, 300μM) or potassium bicarbonate (Fisher Chemical) at 37 C (5% CO_2) for 48h. After 48h, cells were re-stimulated with IL4 (25ng/mL) and anti-CD40 (0.1μg/mL). At 96h, cells were harvested and incubated with fluorochrome-conjugated antibodies (clones) against B220 (RA3–6B2), CD80 (16–10A1), CD86 (GL-1), MHC II (M5/114.15.2), CD11c (N418), F4/80 (BM8), CD4 (GK1.5), CD8 (53–6.7, all from Biolegend) and IgG1(A85–1, BD Biosciences) for 30 minutes at 4 C and collected on an Attune NxT cytometer (Thermo Fisher Scientific). Results were analyzed using Flowjo software (Flowjo LLC). DIDS was reconstituted in 0.1M potassium bicarbonate and added to the cells on day 0 of culture.

Statistics

Statistical significance was determined by Mann-Whitney *U* test for two groups comparison in Prism (GraphPad). One-way ANOVA and two-way ANOVA was used for multiple groups comparison. *p<0.05, **p<0.01, ***p<0.001, ****p<0.0001. Log Rank was used for survival assessment.

RESULTS

Disruption of AID prohibits class switch recombination and retards lupus-like disease progression in BXSB mice

To determine the effect of affinity maturation on the pathogenesis of the lupus-like disease in the BXSB mouse, we employed CRISPR-Cas gene editing to target the *Aicda* gene directly in BXSB zygotes. Due to the complex background genetics of lupus-like disease, we chose this technology to preserve the background genetics of our model. Resulting PCR product sizes are shown in Fig 1A. B lymphocytes were cultured under conditions to induce class switch recombination (34). RT-PCR confirmed that lack of transcript produced in

BXSB.Aicda$^{-/-}$ B lymphocytes under stimulatory conditions (Fig 1B). While wt BXSB B lymphocytes successfully produced a subset of cells expressing IgG1, the BXSB.*Aicda*$^{-/-}$ B lymphocytes remained unswitched (Fig 1C). Sera immunoglobulin levels in BXSB.*Aicda* mice reflect this deficiency as well since these mice lack IgG isotypes and exhibit elevated IgM levels as seen previously in *Aicda*$^{-/-}$ mice (Fig 1D, (22, 29, 35). Male BXSB.*Aicda*$^{-/-}$ exhibited extended lifespans with 100% of mice surviving past 36 weeks while wt BXSB males averaged 15 weeks survival (Fig 1E).

Given that male BXSB.*Aicda*$^{-/-}$ mice survived significantly longer than their wt BXSB counterparts, we sought to phenotype disease progression in these two strains. BXSB lupus-like disease is characterized by elevated sera IgG (Fig 1D), glomerular disease with IgG and C3 deposition and the presence of antinuclear antibodies (ANA) (27, 36–38). Histologic renal pathology seen in BXSB.*Aicda*$^{-/-}$ mice was significantly less than in wt BXSB mice (Fig 2 A, Supplemental Fig 1). The primary renal lesions in wt BXSB mice were membranoproliferative glomerulonephritis and tubular protein casts. Interstitial inflammation was predominantly minimal, and there was no evidence of vasculitis. As BXSB.*Aicda*$^{-/-}$ mice lack IgG, renal immunoglobulin deposition was evaluated using a pan-Ig detection antibody. The mean intensity of glomerular antibody deposition between the two strains did not significantly differ however staining appears to be confined to the mesangial regions in the *Aicda*$^{-/-}$ mice and extends to the glomerular loops in wt BXSB (Fig 2 C,D, Supplemental Fig 2). Despite no measured differences in renal Ig staining, complement component 3 (C3c) deposition was significantly reduced in BXSB.*Aicda*$^{-/-}$ mice compared with wt BXSB mice (Fig 2 E,F).

To evaluate levels of ANA, a pan-Ig antibody was utilized with BXSB.*Aicda*$^{-/-}$ mice exhibiting reduced ANA staining intensity compared to wt BXSB mice (Fig 3A). To assess levels of autoreactive IgM antibodies, ANA intensity was measured using an IgM detection antibody and no differences in labeling intensity were seen in the BXSB.*Aicda*$^{-/-}$ compared with wt BXSB mice (Fig 3A). The predominant pattern seen with the IgM ANA was peri-nuclear localization while the pan-Ig antibody showed principally nuclear staining. (Supplemental Fig 3). Anti-dsDNA antibodies were also quantitated using a pan-Ig antibody as well as an IgM antibody; however; no significant differences were observed with low levels detected in both strains (Fig 3B). Anti-dsDNA ELISPOT showed no differences in bone marrow or splenic plasma cell numbers between the two strains (Fig 3C,D).

Splenic cellularity as assessed using flow cytometry did not vary dramatically between the two strains. B and T lymphocyte percentages were unchanged (Fig 4A). The marginal zone B lymphocyte compartment is known to be reduced in male BXSB mice (27, 38) and this reduction was at least partially restored in mice deficient in AID (Fig 4B). Consistent with other *Aicda*$^{-/-}$ strains (29, 39), the germinal center (GC) B cell compartment was expanded in the BXSB.*Aicda*$^{-/-}$ mice (Fig 4C) however a corresponding increase in T follicular helper (Tfh) cells was not appreciated (Fig 4D). The characteristic expansion of splenic monocytes (CD11b^{+}) did not differ between the two strains (data not shown). Splenic architecture appears distorted in BXSB mice with follicular and germinal center structure difficult to determine; however, AID deficiency resulted in restoration of this architecture with more discernable follicles and germinal centers (Fig 4E).

The ability of BXSB B lymphocytes to mature into plasma cells remained unhampered in the absence of AID

Extrafollicular plasma cell generation is a hallmark of lupus-like disease in BXSB mice (27, 28). We hypothesized that inability to undergo CSR would inhibit plasma cell generation in this model. We found no significant differences in splenic or bone marrow $CD138^+$ populations between wt BXSB and BXSB.*Aicda*$^{-/-}$ (Fig 5A). To determine if this response was intrinsic to B lymphocytes, we performed *in vitro* stimulation for plasma cell generation. We found that both wt BXSB and BXSB.*Aicda*$^{-/-}$ B lymphocytes were able to differentiate into plasma cells under both T-cell independent and T-cell dependent culture conditions (Fig 5B,C). As negative selection during B lymphocyte maturation is thought to lead to apoptosis in low affinity B cells (40), we asked if BXSB.*Aicda*$^{-/-}$ B lymphocytes unable to undergo somatic hypermutation would experience an increase in cell death. We found no increase in apoptosis indicators in the AID-deficient BXSB B lymphocytes (Fig 5D).

Memory B lymphocytes are expanded in AID-deficient BXSB mice

Previously we have reported expansion of B memory cells in *Aicda* deficient mice on the NOD background (29). These memory B cells were also expanded in BXSB.*Aicda*$^{-/-}$ mice with the majority of GC B cells being $CD73^+$ (Fig 6A, B). A change in CD73 MFI on B lymphocytes was not appreciated (Fig 6C). CD73 was also present on a large proportion of $CD4^+$ lymphocytes and Tfh cells (Fig 6D). No change in CD73 MFI was seen on these $CD4^+$ T lymphocytes (Fig 6E). These $CD73^+$ cells were generally associated with the distorted follicular structures seen in wt BXSB, while BXSB.*Aicda*$^{-/-}$ mice showed localization of CD73 mainly in germinal center structures (Fig 6F).

Disruption in repair of AID-induced DNA breaks resulted in minimal attenuation of lupus-like disease in BXSB mice

Double-stranded DNA breaks are initiated by AID during the process of CSR. The RAD51 complex repairs these breaks and inability to mend the DNA damage that occurs during this process results in cell death (34, 41). DIDS, a disulfonated trans-stilbene derivative, has previously been shown to bind to RAD51 and inhibit its function (42). *In vitro* and *in vivo* use of DIDS inhibits DNA break repair and leads to B cell death without evidence of off-target toxicity (20). We recently showed that use of this small molecule inhibitor significantly delayed the development of type 1 diabetes in NOD mice (29). We sought to investigate the effect of DIDS treatment in BXSB model of SLE. *In vitro* assessment of DIDS on B lymphocytes stimulated to undergo CSR showed a dose dependent loss of total B cells and IgG1+ cells (Supplemental Fig 4A, B) without a corresponding decrease in T lymphocytes (Supplemental Fig 4C). Macrophages and dendritic cells (DCs) also showed a dose dependent decrease in cell numbers (Supplemental Fig D) and, while B cell activation markers increased with dosage of the DIDS, (Supplemental Fig 4E–G), DC expression of CD80 and CD86 declined (Supplemental Fig 4H–J). To assess if these results translated *in vivo*, BXSB mice were treated weekly beginning at 6 weeks of age with 50 mg/kg DIDS for 8 injections. mice were euthanized 1 week following the final injection. $CD4^+$ T and B lymphocyte percentages in the spleen were decreased with treatment (Fig 7A), however no

differences were seen in splenic B cell subsets (Fig 7B). GC B cell percentage was unaffected, while the Tfh helper cell population trended towards reduction in the presence of DIDS (Fig 7C, D). The percentage of splenic monocytes was significantly reduced with DIDS administration (Fig 7E). ANA intensity remained consistent between the treated and control groups (Fig 7F) while the circulating IgG levels over the course of the experiment trended towards reduction but did not reach significance (Fig 7G). No change was seen in renal pathology scoring between the two groups (Fig 7H).

DISCUSSION

The disruption of affinity maturation of B lymphocytes through ablation of AID in BXSB mice significantly prolonged survival with decreased renal damage and restoration of splenic architecture. Pathogenic glomerular changes were diminished as was urine protein concentrations. Immune complexes were still present in the *Aicda*$^{-/-}$ mice however complement activation appeared absent. These results suggest that these IgM antibodies lacking SHM are not as adept at activating the inflammatory profile characteristic of lupus nephritis. It is generally accepted that IgG isotypes initiate interferon production fueling renal damage (43) and a potential explanation needing further exploration in this model is the inability of IgM to induce interferon production. While hyperIgM syndrome appears to exist in BXSB.*Aicda*$^{-/-}$ mice as in other AID deficient models (22, 29, 35), anti-nuclear IgM antibody levels do not differ between wt BXSB and BXSB.*Aicda*$^{-/-}$ mice, suggesting no increase in autoreactivity. However, the pattern of Ig and IgM ANA binding is altered between the strains. BXSB.*Aicda*$^{-/-}$ sera presents a cytoplasmic dense fine speckled pattern while wt sera shows a predominately homogeneous nuclear pattern (www.anapatterns.org). This suggests altered antigen affinity which would be of interest to explore further.

While the cellular phenotype of spleens by flow cytometry remained mostly consistent between the two strains, the organization of these cells within the spleen was noticeably altered. GC B cell percentages were increased as previously reported in mice with targeted AID deficiency (29, 35). A corresponding increase in Tfh cells was not observed suggesting that the creation of GC B cells may not be accelerated but perhaps their movement out of this compartment is hampered. A reduction in marginal zone B cells is a consistent change seen in BXSB mice and abrogation of AID restored this population. This lack of detectable changes using traditional flow cytometry in a model with significantly prolonged survival cautions against relying on these markers as an indicator of disease improvement. Further exploration *in situ* revealed despite little change in cellular percentages and numbers, splenic architecture was restored in the spleens of the knockout mice with discernable follicles and germinal centers readily visible. Previously we reported that BXSB mice exhibit a robust extrafollicular response (36) which has also been appreciated in other lupus models (44, 45) as well as suspected in human patients (46). The return to more normal architecture in the AID deficient mice suggests a shift from an extrafollicular response to a germinal center response. However, no differences were seen in plasma cell generation including anti-dsDNA antibody producing plasma cells. BXSB historically has low production of anti-dsDNA antibodies (47) and assay sensitivity may be clouding these results. The possibility exists that while follicular structure is distorted in the wt BXSB mice, the plasma cell

generating interactions between B and T cells are still occurring in a similar manner between the two models. Further studies are needed to investigate this possibility.

BXSB.*Aicda*$^{-/-}$ B lymphocytes expressed increased CD73, a memory B cell marker, which is similar to what we showed in the NOD.*Aicda*$^{-/-}$ model (29). In the NOD model, these CD73^{+} memory B cells exert a protective effect (29). The regulatory role of CD73^{+} memory B cells has yet to be tested in the BXSB model. The literature presents a model in which low affinity GC B cells move into the memory compartment (48). These results support this model as B lymphocytes unable to undergo affinity maturation would presumably remain as lower affinity, increasing the memory B cell compartment.

Given the reduced production of immunoglobulins and increase in the GC B cell compartment in BXSB.*Aicda*$^{-/-}$ mice, we anticipated the generation of plasma cells would be reduced. With diminished auto-reactive antibody levels in these mice, we hypothesized that the *Aicda*$^{-/-}$ B lymphocytes would have limited survival due to low affinity and would not undergo plasma cell differentiation. We did not, however, find a statistically significant drop in the percentage of plasma cells. In fact, we saw that BXSB.*Aicda*$^{-/-}$ B cells were able to differentiate into plasma cells as readily as their wt counterparts *in vitro* and that these cells were not subject to early or late apoptosis. Further study into the generation of these cells and the reduction in pathogenic B lymphocyte development in this model are warranted.

Since disruption of the AID pathway led to significantly improved life span in BXSB mice, targeting this pathway therapeutically may prove beneficial. The small molecule inhibitor of RAD51, 4,4’-Diisothiocyano-2,2’-stilbenedisulfonic acid (DIDS), blocks the ability of B cells to repair the dsDNA breaks induced by AID, causing these cells to undergo early cell death (20). The point of intervention in the pathway is therefore different than targeted knockout of the *Aicda* gene. The NOD model of type 1 diabetes showed success with this therapy and diabetes onset was greatly delayed (29). While the NOD model was successful at a dose of 10mg/kg, BXSB mice were not responsive (data not shown) and a higher dose of 50mg/kg (20) was investigated. While *in vitro* assays with DIDS successfully decreased B lymphocyte populations, we saw no improvement *in vivo* in our mice, namely glomerular pathology was not significantly altered. We did appreciate a decrease in splenic B lymphocytes with a trend towards reduced levels of immunoglobulins. *In vitro* stimulation revealed a toxic effect on DCs and macrophages of BXSB origin not previously reported while the effect of decreasing B lymphocytes and sparing T lymphocytes was consistent with earlier studies (20). We suspect this unexpected effect contributed to the lack of efficacy seen however further exploration is needed. While targeting with the DIDS molecule appeared unsuccessful in diminishing glomerular disease in our mice, we feel our success in genetically targeting of this pathway warrants further exploration for potential therapeutic development

In conclusion, targeting B lymphocyte maturation in the BXSB model alleviated lupus-like nephritis and prolonged survival. One limitation of this work is that only a single founder was used to develop the BXSB.*Aicda*−/− line and thus off-target effects cannot be ruled out. The authors did perform an additional backcross to BXSB to limit this possibility when

creating these mice. Our results are supported by previous work in the MRL model targeting this same molecule (22). Since these two mouse models of SLE vary greatly in disease pathogenesis, these similar findings indicate greater promise that this work could translate to human patients, particularly those with nephritis. Further explorations into ways to target this pathway for the treatment of SLE are warranted.

Supplementary Material

Refer to Web version on PubMed Central for supplementary material.

Acknowledgments

Funding for work reported in this publication was provided by the National Institute of Diabetes and Digestive and Kidney Diseases of the National Institutes of Health under award number K08DK101735 and the National Institute of Arthritis and Musculoskeletal and Skin Diseases of the National Institutes of Health under award number R03AR066787.

REFERENCES

1. Scholz JL, Oropallo MA, Sindhava V, Goenka R, and Cancro MP. 2013 The role of B lymphocyte stimulator in B cell biology: implications for the treatment of lupus. Lupus 22: 350–360. [PubMed: 23553778]
2. Mosak J, and Furie R. 2013 Breaking the ice in systemic lupus erythematosus: belimumab, a promising new therapy. Lupus 22: 361–371. [PubMed: 23553779]
3. Burness CB, and McCormack PL. 2011 Belimumab: in systemic lupus erythematosus. Drugs 71: 2435–2444. [PubMed: 22141386]
4. Wellmann U, Letz M, Herrmann M, Angermuller S, Kalden JR, and Winkler TH. 2005 The evolution of human anti-double-stranded DNA autoantibodies. Proceedings of the National Academy of Sciences of the United States of America 102: 9258–9263. [PubMed: 15968001]
5. van Es JH, Gmelig Meyling FH, van de Akker WR, Aanstoot H, Derksen RH, and Logtenberg T. 1991 Somatic mutations in the variable regions of a human IgG anti-double-stranded DNA autoantibody suggest a role for antigen in the induction of systemic lupus erythematosus. The Journal of experimental medicine 173: 461–470. [PubMed: 1899104]
6. Fava A, and Petri M. 2019 Systemic lupus erythematosus: Diagnosis and clinical management. J Autoimmun 96: 1–13. [PubMed: 30448290]
7. Tsokos GC, Lo MS, Costa Reis P, and Sullivan KE. 2016 New insights into the immunopathogenesis of systemic lupus erythematosus. Nat Rev Rheumatol 12: 716–730. [PubMed: 27872476]
8. Janeway CAT, Paul; Walport Mark; Shlomchik Mark. 2001 Immunobiology. Garland Science, New York and London.
9. Muramatsu M, Nagaoka H, Shinkura R, Begum NA, and Honjo T. 2007 Discovery of activation-induced cytidine deaminase, the engraver of antibody memory. Advances in immunology 94: 1–36. [PubMed: 17560270]
10. Chaudhuri J, Tian M, Khuong C, Chua K, Pinaud E, and Alt FW. 2003 Transcription-targeted DNA deamination by the AID antibody diversification enzyme. Nature 422: 726–730. [PubMed: 12692563]
11. Staszewski O, Baker RE, Ucher AJ, Martier R, Stavnezer J, and Guikema JE. 2011 Activation-induced cytidine deaminase induces reproducible DNA breaks at many non-Ig Loci in activated B cells. Mol Cell 41: 232–242. [PubMed: 21255732]
12. McBride KM, Gazumyan A, Woo EM, Barreto VM, Robbiani DF, Chait BT, and Nussenzweig MC. 2006 Regulation of hypermutation by activation-induced cytidine deaminase phosphorylation. Proc Natl Acad Sci U S A 103: 8798–8803. [PubMed: 16723391]

13. Robbiani DF, Bunting S, Feldhahn N, Bothmer A, Camps J, Deroubaix S, McBride KM, Klein IA, Stone G, Eisenreich TR, Ried T, Nussenzweig A, and Nussenzweig MC. 2009 AID produces DNA double-strand breaks in non-Ig genes and mature B cell lymphomas with reciprocal chromosome translocations. Mol Cell 36: 631–641. [PubMed: 19941823]
14. Shinohara A, Ogawa H, and Ogawa T. 1992 Rad51 protein involved in repair and recombination in S. cerevisiae is a RecA-like protein. Cell 69: 457–470. [PubMed: 1581961]
15. Sung P, and Robberson DL. 1995 DNA strand exchange mediated by a RAD51-ssDNA nucleoprotein filament with polarity opposite to that of RecA. Cell 82: 453–461. [PubMed: 7634335]
16. Daboussi F, Dumay A, Delacote F, and Lopez BS. 2002 DNA double-strand break repair signalling: the case of RAD51 post-translational regulation. Cell Signal 14: 969–975. [PubMed: 12359302]
17. Kawabata M, Kawabata T, and Nishibori M. 2005 Role of recA/RAD51 family proteins in mammals. Acta Med Okayama 59: 1–9. [PubMed: 15902993]
18. Thacker J 2005 The RAD51 gene family, genetic instability and cancer. Cancer Lett 219: 125–135. [PubMed: 15723711]
19. Suwaki N, Klare K, and Tarsounas M. 2011 RAD51 paralogs: roles in DNA damage signalling, recombinational repair and tumorigenesis. Semin Cell Dev Biol 22: 898–905. [PubMed: 21821141]
20. Lamont KR, Hasham MG, Donghia NM, Branca J, Chavaree M, Chase B, Breggia A, Hedlund J, Emery I, Cavallo F, Jasin M, Ruter J, and Mills KD. 2013 Attenuating homologous recombination stimulates an AID-induced antileukemic effect. J Exp Med 210: 1021–1033. [PubMed: 23589568]
21. White CA, Seth Hawkins J, Pone EJ, Yu ES, Al-Qahtani A, Mai T, Zan H, and Casali P. 2011 AID dysregulation in lupus-prone MRL/Fas(lpr/lpr) mice increases class switch DNA recombination and promotes interchromosomal c-Myc/IgH loci translocations: modulation by HoxC4. Autoimmunity 44: 585–598. [PubMed: 21585311]
22. Jiang C, Foley J, Clayton N, Kissling G, Jokinen M, Herbert R, and Diaz M. 2007 Abrogation of lupus nephritis in activation-induced deaminase-deficient MRL/lpr mice. J Immunol 178: 7422–7431. [PubMed: 17513793]
23. Jiang C, Zhao ML, Scearce RM, and Diaz M. 2011 Activation-induced deaminase-deficient MRL/lpr mice secrete high levels of protective antibodies against lupus nephritis. Arthritis and rheumatism 63: 1086–1096. [PubMed: 21225690]
24. Chen L, Guo L, Tian J, Zheng B, and Han S. 2010 Deficiency in activation-induced cytidine deaminase promotes systemic autoimmunity in lpr mice on a C57BL/6 background. Clinical and experimental immunology 159: 169–175. [PubMed: 19922498]
25. Pisitkun P, Deane JA, Difilippantonio MJ, Tarasenko T, Satterthwaite AB, and Bolland S. 2006 Autoreactive B cell responses to RNA-related antigens due to TLR7 gene duplication. Science 312: 1669–1672. [PubMed: 16709748]
26. Subramanian S, Tus K, Li QZ, Wang A, Tian XH, Zhou J, Liang C, Bartov G, McDaniel LD, Zhou XJ, Schultz RA, and Wakeland EK. 2006 A Tlr7 translocation accelerates systemic autoimmunity in murine lupus. Proc Natl Acad Sci U S A 103: 9970–9975. [PubMed: 16777955]
27. McPhee CG, Bubier JA, Sproule TJ, Park G, Steinbuck MP, Schott WH, Christianson GJ, Morse HC 3rd, and Roopenian DC. 2013 IL-21 Is a Double-Edged Sword in the Systemic Lupus Erythematosus-like Disease of BXSB.Yaa Mice. J Immunol 27: 27.
28. Jain S, Park G, Sproule TJ, Christianson GJ, Leeth CM, Wang H, Roopenian DC, and Morse HC 3rd. 2016 Interleukin 6 Accelerates Mortality by Promoting the Progression of the Systemic Lupus Erythematosus-Like Disease of BXSB.Yaa Mice. PLoS One 11: e0153059. [PubMed: 27050763]
29. Ratiu JJ, Racine JJ, Hasham MG, Wang Q, Branca JA, Chapman HD, Zhu J, Donghia N, Philip V, Schott WH, Wasserfall C, Atkinson MA, Mills KD, Leeth CM, and Serreze DV. 2017 Genetic and Small Molecule Disruption of the AID/RAD51 Axis Similarly Protects Nonobese Diabetic Mice from Type 1 Diabetes through Expansion of Regulatory B Lymphocytes. J Immunol 198: 4255–4267. [PubMed: 28461573]

30. McPhee CG, Bubier JA, Sproule TJ, Park G, Steinbuck MP, Schott WH, Christianson GJ, Morse HC 3rd, and Roopenian DC. 2013 IL-21 is a double-edged sword in the systemic lupus erythematosus-like disease of BXSB.Yaa mice. Journal of immunology 191: 4581–4588.

31. Mu Q, Zhang H, Liao X, Lin K, Liu H, Edwards MR, Ahmed SA, Yuan R, Li L, Cecere TE, Branson DB, Kirby JL, Goswami P, Leeth CM, Read KA, Oestreich KJ, Vieson MD, Reilly CM, and Luo XM. 2017 Control of lupus nephritis by changes of gut microbiota. Microbiome 5: 73. [PubMed: 28697806]

32. Weening JJ, D'Agati VD, Schwartz MM, Seshan SV, Alpers CE, Appel GB, Balow JE, Bruijn JA, Cook T, Ferrario F, Fogo AB, Ginzler EM, Hebert L, Hill G, Hill P, Jennette JC, Kong NC, Lesavre P, Lockshin M, Looi LM, Makino H, Moura LA, and Nagata M. 2004 The classification of glomerulonephritis in systemic lupus erythematosus revisited. J Am Soc Nephrol 15: 241–250. [PubMed: 14747370]

33. Taddeo A, Khodadadi L, Voigt C, Mumtaz IM, Cheng Q, Moser K, Alexander T, Manz RA, Radbruch A, Hiepe F, and Hoyer BF. 2015 Long-lived plasma cells are early and constantly generated in New Zealand Black/New Zealand White F1 mice and their therapeutic depletion requires a combined targeting of autoreactive plasma cells and their precursors. Arthritis Res Ther 17: 39. [PubMed: 25889236]

34. Hasham MG, Snow KJ, Donghia NM, Branca JA, Lessard MD, Stavnezer J, Shopland LS, and Mills KD. 2012 Activation-induced cytidine deaminase-initiated off-target DNA breaks are detected and resolved during S phase. J Immunol 189: 2374–2382. [PubMed: 22826323]

35. Muramatsu M, Kinoshita K, Fagarasan S, Yamada S, Shinkai Y, and Honjo T. 2000 Class switch recombination and hypermutation require activation-induced cytidine deaminase (AID), a potential RNA editing enzyme. Cell 102: 553–563. [PubMed: 11007474]

36. McPhee CG, Sproule TJ, Shin DM, Bubier JA, Schott WH, Steinbuck MP, Avenesyan L, Morse HC 3rd, and Roopenian DC. 2011 MHC class I family proteins retard systemic lupus erythematosus autoimmunity and B cell lymphomagenesis. J Immunol 187: 4695–4704. [PubMed: 21964024]

37. Bubier JA, Bennett SM, Sproule TJ, Lyons BL, Olland S, Young DA, and Roopenian DC. 2007 Treatment of BXSB-Yaa mice with IL-21R-Fc fusion protein minimally attenuates systemic lupus erythematosus. Ann N Y Acad Sci 1110: 590–601. [PubMed: 17911475]

38. Bubier JA, Sproule TJ, Foreman O, Spolski R, Shaffer DJ, Morse HC 3rd, Leonard WJ, and Roopenian DC. 2009 A critical role for IL-21 receptor signaling in the pathogenesis of systemic lupus erythematosus in BXSB- Yaa mice. Proc Natl Acad Sci U S A.

39. Dahlberg CI, He M, Visnes T, Torres ML, Cortizas EM, Verdun RE, Westerberg LS, Severinson E, and Strom L. 2014 A novel mouse model for the hyper-IgM syndrome: a spontaneous activation-induced cytidine deaminase mutation leading to complete loss of Ig class switching and reduced somatic hypermutation. J Immunol 193: 4732–4738. [PubMed: 25252954]

40. Anderson SM, Khalil A, Uduman M, Hershberg U, Louzoun Y, Haberman AM, Kleinstein SH, and Shlomchik MJ. 2009 Taking advantage: high-affinity B cells in the germinal center have lower death rates, but similar rates of division, compared to low-affinity cells. J Immunol 183: 7314–7325. [PubMed: 19917681]

41. Hasham MG, Donghia NM, Coffey E, Maynard J, Snow KJ, Ames J, Wilpan RY, He Y, King BL, and Mills KD. 2010 Widespread genomic breaks generated by activation-induced cytidine deaminase are prevented by homologous recombination. Nature immunology 11: 820–826. [PubMed: 20657597]

42. Ishida T, Takizawa Y, Kainuma T, Inoue J, Mikawa T, Shibata T, Suzuki H, Tashiro S, and Kurumizaka H. 2009 DIDS, a chemical compound that inhibits RAD51-mediated homologous pairing and strand exchange. Nucleic Acids Res 37: 3367–3376. [PubMed: 19336413]

43. Lech M, and Anders HJ. 2013 The pathogenesis of lupus nephritis. J Am Soc Nephrol 24: 1357–1366. [PubMed: 23929771]

44. Odegard JM, Marks BR, DiPlacido LD, Poholek AC, Kono DH, Dong C, Flavell RA, and Craft J. 2008 ICOS-dependent extrafollicular helper T cells elicit IgG production via IL-21 in systemic autoimmunity. J Exp Med 205: 2873–2886. [PubMed: 18981236]

45. Rankin AL, Guay H, Herber D, Bertino SA, Duzanski TA, Carrier Y, Keegan S, Senices M, Stedman N, Ryan M, Bloom L, Medley Q, Collins M, Nickerson-Nutter C, Craft J, Young D, and

Dunussi-Joannopoulos K. 2012 IL-21 receptor is required for the systemic accumulation of activated B and T lymphocytes in MRL/MpJ-Fas(lpr/lpr)/J mice. J Immunol 188: 1656–1667. [PubMed: 22231702]

46. Jenks SA, Cashman KS, Woodruff MC, Lee FE, and Sanz I. 2019 Extrafollicular responses in humans and SLE. Immunol Rev 288: 136–148. [PubMed: 30874345]
47. Li L, Nukala S, Du Y, Han J, Liu K, Hutcheson J, Pathak S, Li Q, and Mohan C. 2012 Murine lupus strains differentially model unique facets of human lupus serology. Clin Exp Immunol 168: 178–185. [PubMed: 22471278]
48. Malkiel S, Barlev AN, Atisha-Fregoso Y, Suurmond J, and Diamond B. 2018 Plasma Cell Differentiation Pathways in Systemic Lupus Erythematosus. Front Immunol 9: 427. [PubMed: 29556239]

Key Points

- CSR and SHM are required for the progression of lupus nephritis in BXSB mice
- $AID^{-/-}$ BXSB mice have prolonged survival with improved renal function

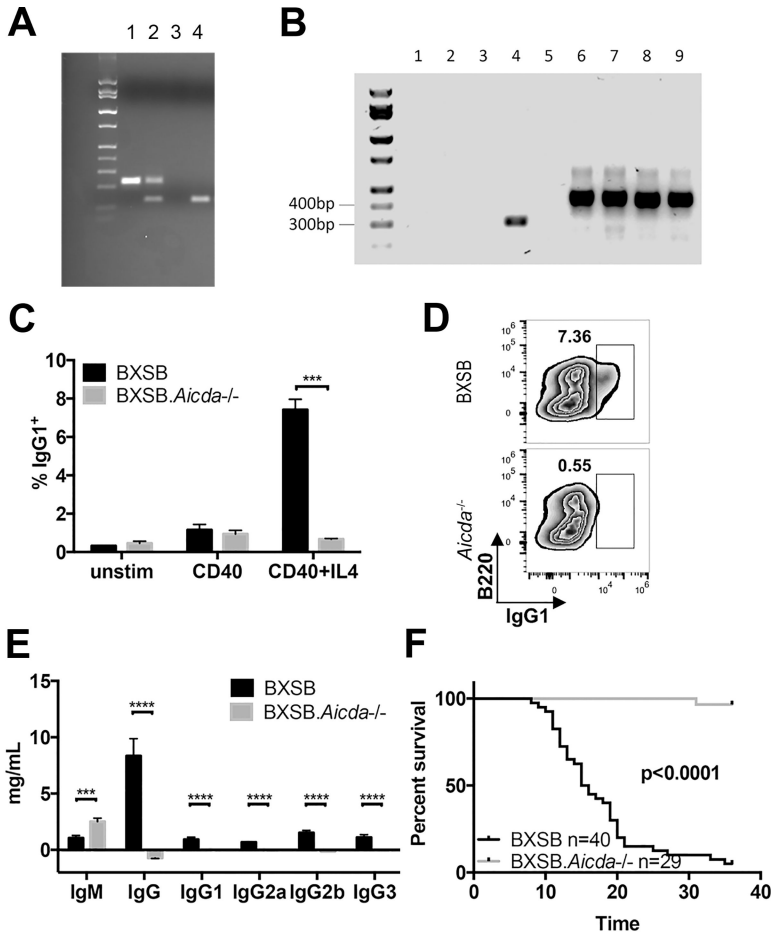

FIGURE 1.

Disruption of *Aicda* extends survival in BXSB mice. (**A**) CRISPR-Cas deletion shortens *Aicda* in BXSB mice. Lane 1 = wt, lane 2 = heterozygous, lane 3 = water, lane 4 = homozygous mutation. (**B**) Representative data of AID expression using RT PCR upon stimulation of B cells *in vitro*. Lane 1: water, Lane 2–5: *Aicda,* Lane 6–9: *Gapdh*, Lane 2,6: BXSB unstimulated, Lane 3,7: BXSB.*Aicda*$^{-/-}$ unstimulated, Lane 4,8: BXSB CD40+IL4 stimulated, Lane 5,9: BXSB CD40+IL4 stimulated. (**C**) *In vitro* stimulation of B cells to induce class switch to IgG1 is abrogated in BXSB.*Aicda*$^{-/-}$ mice. The percentage of IgG1^{+} cells in the viable cell population were shown (n=3 for both groups). Data are presented as mean±SEM. Unpaired t test was used for statistical analysis. ***P<0.001. (**D**) Representative FACS zebra plots of (C) data. (**E**) IgM and IgG isotypes present in sera from 12-week-old BXSB (n=15) and BXSB.*Aicda*$^{-/-}$ males (n=11). Data are presented as mean ±SEM. Statistical significance was determined by Mann-Whitney *U* test. ***P<0.001, ****p<0.0001. (**F**) Survival curve for BXSB and BXSB.*Aicda*$^{-/-}$ males. Log-rank test was used for statistical analysis.

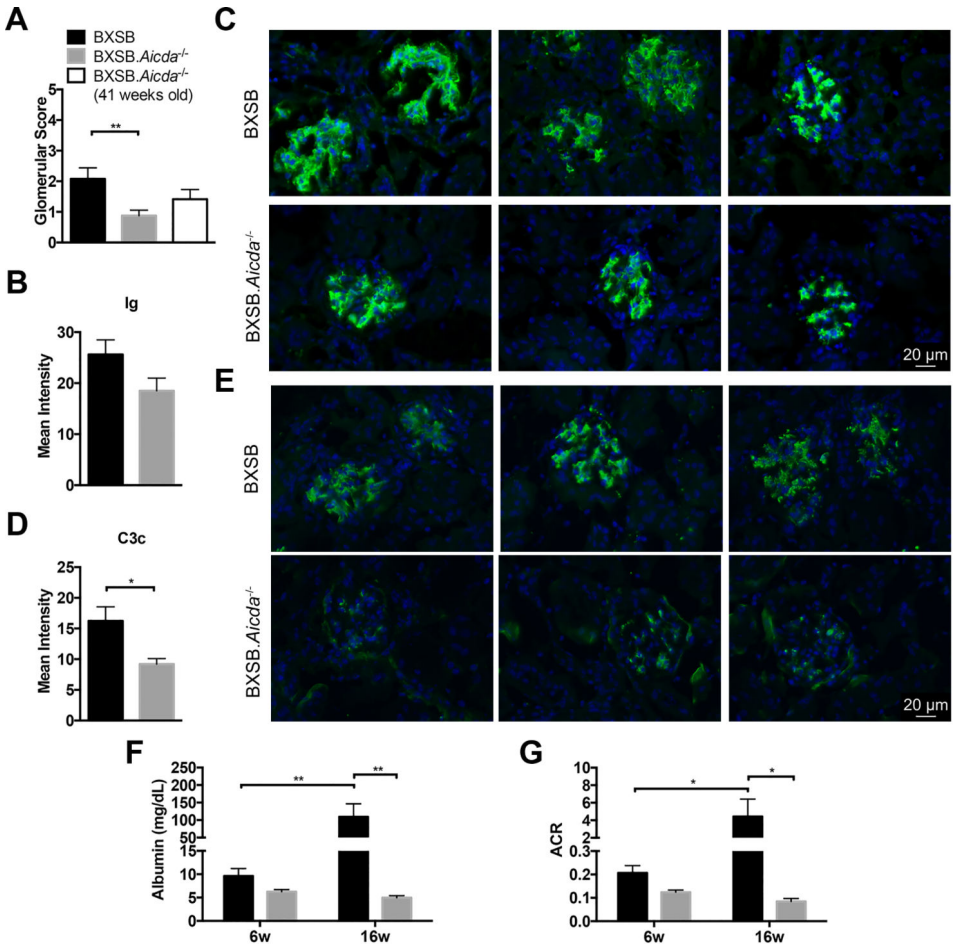

FIGURE 2.

Complement activation was attenuated and kidney function improved in the absence of AID. (**A**) Glomeruli scores were compared between 12-week-old BXSB (n=12), 12-week-old BXSB.*Aicda*$^{-/-}$ (n=16) and 41-week-old BXSB.*Aicda*$^{-/-}$ (n=12) mice. (**B**-**E**) Kidney images from 12-week-old BXSB (n=5) and BXSB.*Aicda*$^{-/-}$ (n=5) mice. Ig (Green), C3c (Green) and DAPI (Blue). Images were evaluated for mean intensity in **B** and **D**. Representative Ig staining images were shown in **C** and C3c staining was shown in **E** (magnification 400X). Statistical significance was determined by Mann-Whitney *U* test. *p<0.05, **p<0.01. (**F**,**G**) Free catch urine samples were collected from 6-week-old and 16-week-old BXSB (n=8) and BXSB.*Aicda*$^{-/-}$ (n=6) mice. Albuminuria is shown in (F) and the albumin to creatinine ratio (ACR) is shown in (G). Statistical significance was determined by Two-way ANOVA. *p<0.05, **p<0.01.

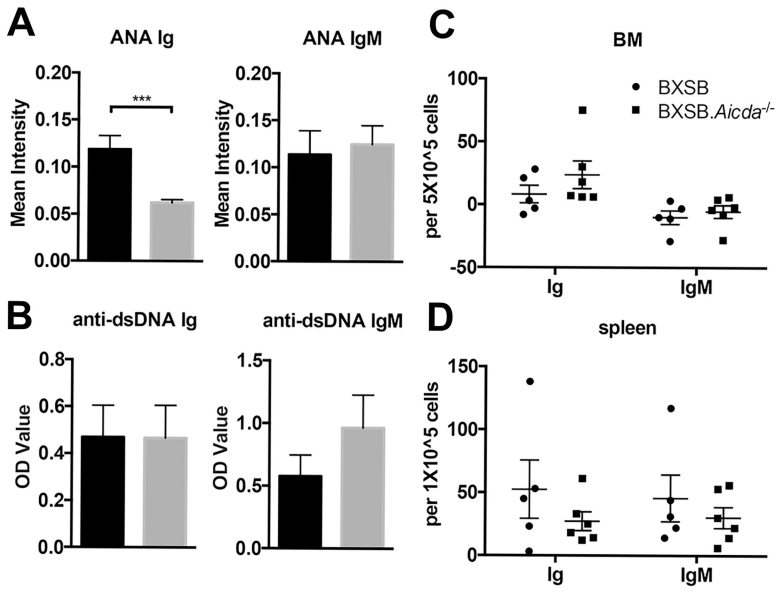

FIGURE 3.

Levels of circulating anti-nuclear antibodies were reduced in AID deficient BXSB mice. (**A**) Sera ANA intensity detection of pan-Ig and IgM autoantibodies in 12-week-old BXSB (n=15) and BXSB.*Aicda*$^{-/-}$ (n=11) mice. (**B**) Sera anti-dsDNA autoantibody detection for pan-Ig and IgM isotypes in these same mice. Anti-dsDNA plasma cell ELISPOT analysis of bone marrow (**C**) and spleen (**D**) from 12-week-old BXSB (n=5) and BXSB.*Aicda*$^{-/-}$ (n=6) mice. Spot numbers in C and E are normalized to control wells. Data are presented as mean ±SEM. Statistical significance was determined by Mann-Whitney *U* test. ***p<0.001.

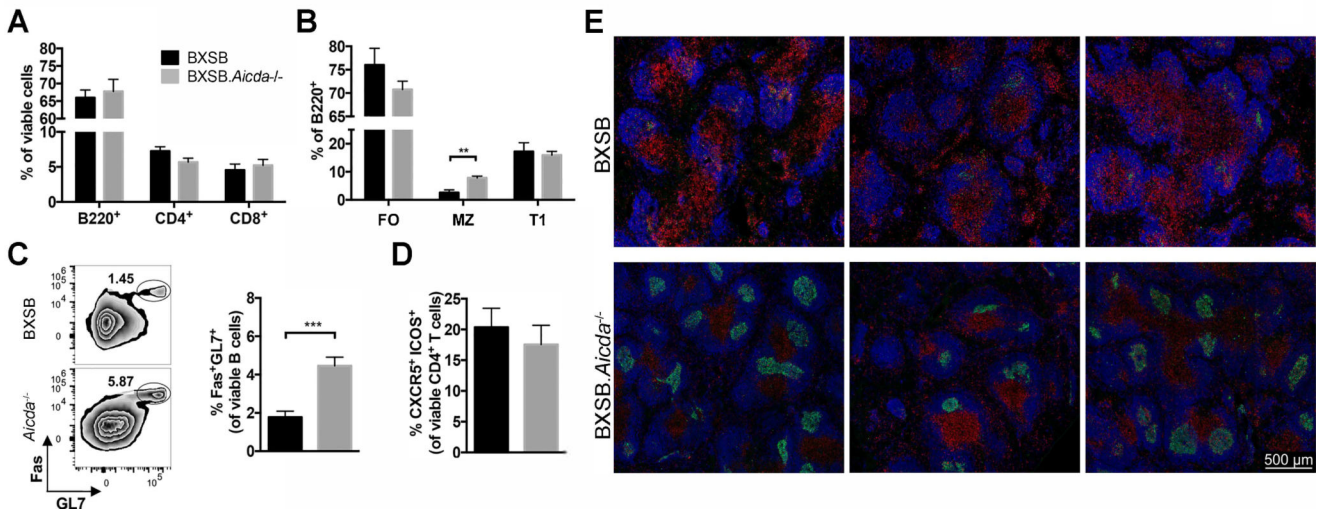

FIGURE 4.

Marginal zone B cell depletion and germinal center integrity restored in BXSB.*Aicda*$^{-/-}$ mice. Splenocytes of 12-week-old BXSB (n=7) and BXSB.*Aicda*$^{-/-}$ (n=9) males were analyzed. (**A**) The percentages of B220^{+}, CD4^{+} and CD8^{+} cells in the viable cell population were compared between wt and *Aicda*$^{-/-}$ mice. (**B**) The percentages of follicular (FO, CD23^{+} CD21^{+}), marginal zone (MZ, CD23$^{low/-}$ CD21^{+}) and transitional 1 (T1, CD23^{-} CD21^{-}) B cells in the B lymphocyte population are shown. (**C**) Representative flow cytometric zebra plots showing the percentage of germinal center (GC) B cells (Fas^{+} GL7^{+}) in the viable B lymphocyte population with summary data shown on the right. (**D**) The percentage of T_{FH} cells (CXCR5^{+} ICOS^{+}). (**E**) Representative confocal images showing the follicles in the spleen. Blue: B220, Green: GL7 and Red: CD4. Data are presented as mean ±SEM. Statistical significance was determined by Mann-Whitney *U* test. **p<0.01, ***p<0.001. Results are representative for at least 3 independent experiments.

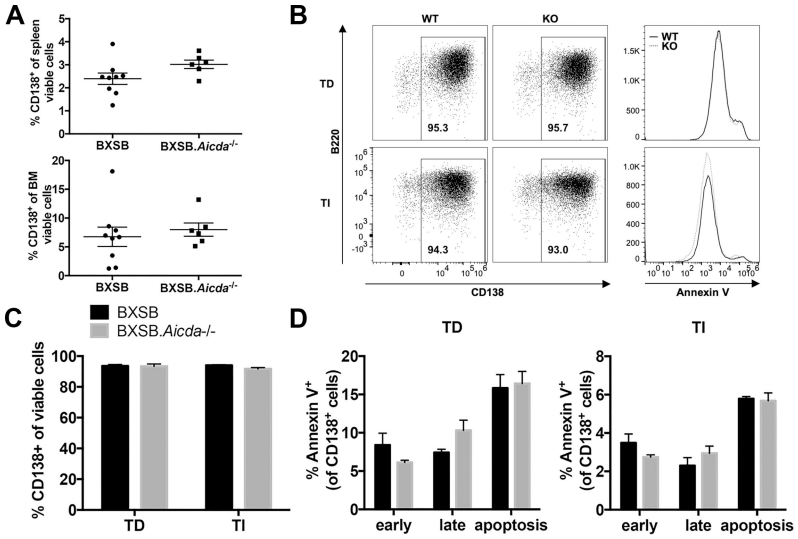

FIGURE 5.

No effect on plasma cell generation both *in vivo* and *in vitro* in the absence of AID. (**A**) The percentage of plasma cells ($CD138^+$) in either viable splenocytes or viable bone marrow cells were compared between 12-week-old BXSB (n=9) and BXSB.$Aicda^{-/-}$ (n=6) males. (**B**-**D**) Enriched B lymphocytes from 8-week-old BXSB (n=3) and BXSB.$Aicda^{-/-}$ (n=3) males were stimulated to differentiate into plasma cells either with anti-CD40 for T cell-dependent (TD) response or LPS for T cell-independent (TI) response. Representative plasma cell staining in viable cells and Annexin V staining in $CD138^+$ cells is shown in **B** and data are summarized in **C** and **D**. Early and late apoptosis were differentiated by Annexin V and 7-AAD respectively. Early apoptosis (early, Annexin $V^+7\text{-}AAD^-$), late apoptosis (late, Annexin $V^+7\text{-}AAD^+$) and all apoptosis (apoptosis, Annexin V^+) were compared in **D**. Data are presented as mean±SEM. Statistical significance was determined by Mann-Whitney *U* test. Results are representative for at least 3 independent experiments.

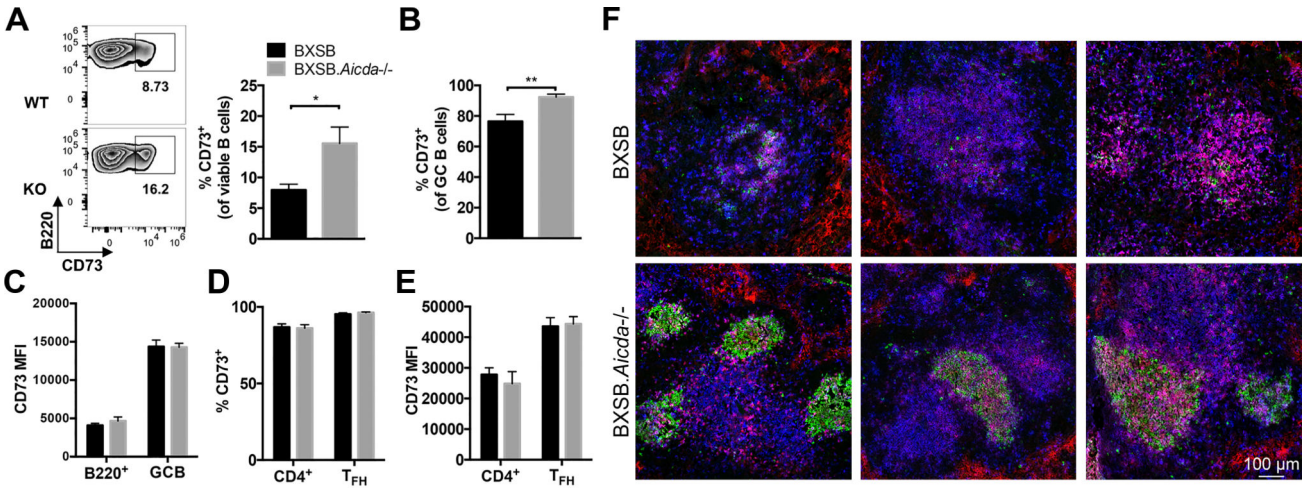

FIGURE 6.

Memory B cell population expanded in BXSB.*Aicda*$^{-/-}$ mice. Splenocytes of 12-week-old BXSB (n=6) and BXSB.*Aicda*$^{-/-}$ (n=6) males were analyzed. (**A**) Representative flow cytometric zebra plots showing the percentage of CD73^{+} in the viable B lymphocyte population with summary data shown on the right. (**B**) The percentages of CD73^{+} GC B cells. (**C**) MFI of CD73 on B cells and GC B cells. (**D**) The percentages of CD73^{+} cells in the viable CD4^{+} and T_{FH} (PD-1^{+}ICOS^{+}) cell populations. (**E**) MFI of CD73 in CD4^{+} cells and T_{FH} cells. (**F**) Representative confocal images of spleen showing the distribution of CD73. Blue: CD4, Green: GL7 and Red: CD73. Data are presented as mean±SEM. Statistical significance was determined by Mann-Whitney *U* test. *p<0.05, **p<0.01. Results are representative for at least 3 independent experiments.

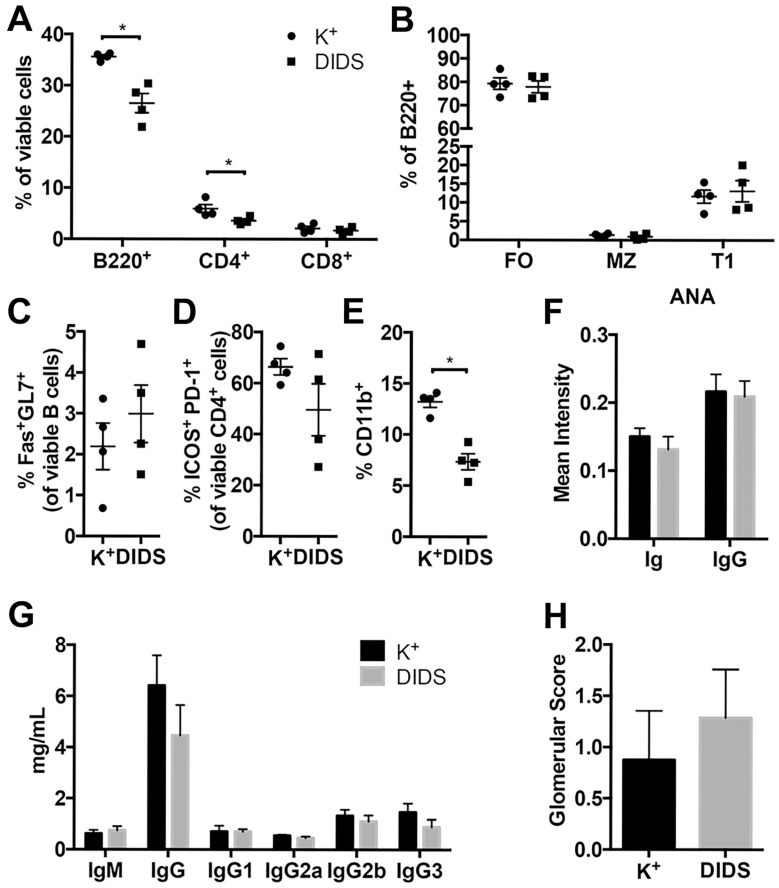

FIGURE 7.

Blocking DNA repair of attempted CSR does not significantly alter the course of SLE-like disease in BXSB mice. (**A**-**E**) 6 week old BXSB males received either 50mg/Kg DIDS (n=4) or vehicle (K^+, potassium bicarbonate, n=4) weekly for 8 injections. Mice were euthanized one week after final injection. Splenocytes were analyzed using flow cytometry and data are representative for 3 independent experiments. (**A**) Percentage of lymphocyte populations (**B**) Percentages of B cell populations (gating strategy the same as in Fig 4). (**C**) Percentage of germinal center B cells (**D**) Percentage of Tfh cells (**E**) Percentage of monocytes (**F**-**H**) 50mg/Kg DIDS (n=7) or vehicle (n=8) treated mice were analyzed. (**G**) Immunoglobulin isotypes in sera. (**F**) Mean intensity of ANA staining for pan Ig and IgG isotypes. Glomerular scores were evaluated in (**H**). Data are presented as mean±SEM. Statistical significance was determined by Mann-Whitney *U* test. *p<0.05.